

## Langevin approach to a chemical wave front: Selection of the propagation velocity in the presence of internal noise

A. Lemarchand,<sup>1</sup> A. Lesne,<sup>1</sup> and M. Mareschal<sup>2</sup>

<sup>1</sup>Laboratoire de Physique Théorique des Liquides, CNRS URA 765, Université Pierre et Marie Curie, 4 Place Jussieu, F-75252 Paris Cedex 05, France

<sup>2</sup>Département de Chimie-Physique, Université Libre de Bruxelles, Campus Plaine, Boulevard du Triomphe, B-1050 Bruxelles, Belgium

(Received 31 October 1994; revised manuscript received 23 January 1995)

The reaction-diffusion equation associated with the Fisher chemical model  $A + B \rightarrow 2A$  admits wave-front solutions by replacing an unstable stationary state with a stable one. The deterministic analysis concludes that their propagation velocity is not prescribed by the dynamics. For a large class of initial conditions the velocity which is spontaneously selected is equal to the minimum allowed velocity  $v_{\min}$ , as predicted by the marginal stability criterion. In order to test the relevance of this deterministic description we investigate the macroscopic consequences, on the velocity and the width of the front, of the intrinsic stochasticity due to the underlying microscopic dynamics. We solve numerically the Langevin equations, deduced analytically from the master equation within a system size expansion procedure. We show that the mean profile associated with the stochastic solution propagates faster than the deterministic solution at a velocity up to 25% greater than  $v_{\min}$ .

PACS number(s): 47.70.Fw, 82.20.Mj, 82.20.Fd, 05.40.+j

### I. INTRODUCTION

Spatiotemporal organization in inert and living systems offers a large variety of mechanisms among which wave-front propagation appears as a simple and rich example. In the specific case of a wave front replacing an unstable stationary uniform state with a stable one, the propagation velocity is not imposed by the dynamics, and the mechanisms governing its selection have been extensively studied.

Fisher [1] originally built a reaction-diffusion model to describe the spread of a favored genetic trait through a population. At the same time, Kolmogorov, Petrovsky, and Piskunov [2] worked independently on the same reaction-diffusion equation, which will be further referred to as the FKPP equation. Since then, the FKPP equation found various applications in biology [3] as well as in the description of various phenomena such as flame propagation [4,5], phase separation of polymer melts [6], or chemical wave fronts in nonlinear chemistry [7–12]. Several macroscopic studies [13–16] have led to the conclusion that a continuum of possible propagation velocities greater than a minimum value exists. Moreover, according to marginal stability analysis [13,15], sufficiently steep initial profiles have been shown to relax to the front, propagating at the minimum allowed velocity.

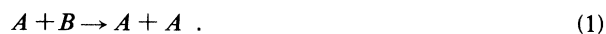
In this paper, our goal is to test the validity of the macroscopic deterministic description when some effects of the underlying microscopic dynamics are taken into account. More particularly, we will be concerned with the possibility of a modification of the minimal velocity selection mechanism by internal fluctuations. In order to analyze these questions, we have set up a numerical investigation of a front-propagating solution in the presence of internal noise. This consists in solving the Langevin

equations [17–19] associated with the FKPP model [1,2] in the frame moving along with the front. Both the front width and velocity can be determined with and without noise. In a similar context, a direct modeling of Turing pattern formation has recently been performed [20] using a lattice-gas cellular automaton: a modification of the stability regions, due to internal noise, has been reported.

The paper is organized as follows. In the next section, the results of the marginal stability analysis specific to the case of the Fisher reaction-diffusion model are recalled. Then, the Langevin equations associated with this model are deduced from the master equation in Sec. III. Technical details about the numerical integration scheme are given in the Appendix. Results are discussed in Sec. IV, while some conclusions are drawn in Sec. V.

### II. SOME RESULTS OF THE MACROSCOPIC THEORY

We consider an infinite two-dimensional (2D) medium containing two chemical species  $A$  and  $B$ , which may diffuse with an identical coefficient  $D$  and react according to the following autocatalytic reaction of rate constant  $\kappa$ :



Due to the reaction and diffusion processes, the concentration of a given species or number of particles of this species per unit surface varies with space  $(x,y)$  and time  $t$ .

From a macroscopic point of view,  $\bar{A}(x,y,t)$  and  $\bar{B}(x,y,t)$  respectively denote the local concentrations of particles  $A$  and  $B$ . At time  $t=0$ , the total concentration  $\bar{C}(x,y,t) = \bar{A}(x,y,t) + \bar{B}(x,y,t)$  is supposed to be spatially homogeneous and equal to the constant  $\bar{C}$ . Since the species  $A$  and  $B$  diffuse with the same diffusion

coefficient and since the chemical reaction given in Eq. (1) does not modify the total number of particles, the total concentration remains constant; that is, whatever  $x$ ,  $y$ , and  $t$ ,

$$\bar{C}(x, y, t) = \bar{C}. \quad (2)$$

Defining respectively the local fractions of particles  $A$  and  $B$  at time  $t$  by  $\bar{a} \equiv \bar{a}(x, y, t) = \bar{A}(x, y, t) / \bar{C}$  and  $\bar{b} \equiv \bar{b}(x, y, t) = \bar{B}(x, y, t) / \bar{C}$ , it follows that

$$\bar{a} + \bar{b} = 1, \quad (3)$$

whatever  $x$ ,  $y$ , and  $t$ . The deterministic evolution of the system hence reduces to the following reaction-diffusion equation:

$$\frac{\partial \bar{a}}{\partial t} = K\bar{a}(1 - \bar{a}) + D \left[ \frac{\partial^2 \bar{a}}{\partial x^2} + \frac{\partial^2 \bar{a}}{\partial y^2} \right], \quad (4)$$

where  $K$  is given by

$$K = \kappa \bar{C}. \quad (5)$$

It is worth mentioning that the reaction-diffusion equation (4) only depends on the two parameters  $K$  and  $D$ , so that the macroscopic behaviors of two different systems labeled 1 and 2 are identical, provided their chemical rate constants, total concentrations, and diffusion coefficients obey the following relations:

$$\kappa_1 \bar{C}_1 = \kappa_2 \bar{C}_2, \quad D_1 = D_2. \quad (6)$$

As will be seen in next section, let us mention that the stochastic behaviors of these two systems are different.

Since the pioneering works of Fischer [1] and Kolmogorov, Petrovsky, and Piskunov [2] in 1937, the FKPP equation has been extensively studied. It is well known [13–15] that, for adequate initial conditions, it admits uniformly translating solutions  $\bar{a}(x - vt)$ , independent of  $y$ , moving in the direction  $x$  with a constant velocity  $v$  and replacing the unstable uniform and stationary state  $\bar{a} = 0$  by the stable state  $\bar{a} = 1$ . An essential feature of Eq. (4) is the existence of such stable wave-front solutions for any propagation velocity  $v$  greater than a minimum value  $v_{\min}$  given by

$$v_{\min} = 2\sqrt{KD}, \quad (7)$$

which satisfies the marginal stability criterion [15].

It has also been proven [13,15] that a large class of sufficiently steep profiles, including a step function, evolve in time to the stable solution  $\bar{a}(x - v_{\min}t)$ , which propagates with the minimum allowed velocity. This wave front appears as stationary in the frame moving at velocity  $v_{\min}$ .

As a matter of fact, numerical solutions of the deterministic reaction-diffusion equation (4) always relax to the front, which propagates at the minimum velocity. In particular, fronts propagating initially with a higher velocity seem to be slowed down to the marginal one by small but unavoidable perturbations induced by the finite precision of the numerical computation. The analytical expression of the profile propagating with the minimum velocity is not known, but an approximate value  $p$  of the

steepness at the inflection point can be used to define a front width [3] as

$$e_{\min} = \frac{1}{|p|} \approx 8 \left( \frac{D}{K} \right)^{1/2}. \quad (8)$$

### III. INTERNAL FLUCTUATION DESCRIPTION THROUGH THE LANGEVIN FORMALISM

The description of reaction-diffusion systems by deterministic equations such as Eq. (4) does not take into account the internal fluctuations that are generated by the underlying microscopic dynamics. In critical situations or for a system that is not structurally stable, it is well known [16–19] that internal noise is able to induce observable deviations from the deterministic or mean-field behavior. In the specific case of a wave front propagating into an unstable stationary state, the existence of a continuum of possible propagation velocities may enhance the sensitivity to fluctuations, and it may be asked whether internal noise influences the selection of a particular propagation velocity. In this spirit, we have already performed microscopic simulations of the FKPP model adapting two different numerical methods, the direct simulation Monte Carlo method [10], originally built by Bird [21] in the context of dilute gases, and a lattice gas cellular automaton model [11,12] first introduced by Hardy, de Pazzis, and Pomeau [22]. In both cases, the deviations that we observed between the mean properties of the simulated front and the deterministic predictions were too small compared to the error bars of the simulation to be significant.

In the present study, we have chosen an intermediate level of description, the so-called mesoscopic level at which the local concentrations  $A(x, y, t)$  and  $B(x, y, t)$  of particles  $A$  and  $B$  are treated as random variables. Their evolution is described through a Langevin equation obtained from the deterministic equation for variable  $\alpha$  ( $\alpha = A, B$ ) by adding a random force [19]  $F_\alpha(x, y, t)$ , which is supposed to mimic all the effects of the microscopic dynamics. Our goal here is to take advantage of the reduction of actual microscopic dynamics to the simplified Langevin formulation to favor a direct comparison with the deterministic results and to make more precise the role of internal fluctuations on the selection of a propagation velocity.

As in the deterministic case, the initial conditions are such that the total local concentration  $C(x, y, t) = A(x, y, t) + B(x, y, t)$  is initially homogeneous and equal to the constant  $\bar{C}$ . The initial conditions obey

$$C(x, y, 0) = \bar{C}. \quad (9)$$

The local fractions of particles  $A$  and  $B$  are now respectively defined as

$$a \equiv a(x, y, t) = \frac{A(x, y, t)}{\bar{C}}, \quad b \equiv b(x, y, t) = \frac{B(x, y, t)}{\bar{C}}, \quad (10)$$

but they do not fluctuate in the same way and the Langevin description cannot be reduced to a single equa-

tion as was the case in the deterministic analysis. Choosing the random variables  $a$  and  $c$ , with  $c$  defined as

$$c = a + b, \quad (11)$$

the Langevin approach formally leads to the following stochastic differential equations:

$$\frac{\partial a}{\partial t} = Ka(c - a) + D \left[ \frac{\partial^2 a}{\partial x^2} + \frac{\partial^2 a}{\partial y^2} \right] + F_a(x, y, t), \quad (12a)$$

$$\frac{\partial c}{\partial t} = D \left[ \frac{\partial^2 c}{\partial x^2} + \frac{\partial^2 c}{\partial y^2} \right] + F_c(x, y, t), \quad (12b)$$

where the mean value of the forces vanishes according to

$$\langle F_a(x, y, t) \rangle = \langle F_c(x, y, t) \rangle = 0,$$

$$\text{whatever } x, y, \text{ and } t. \quad (13)$$

The variable  $c$  is not affected by the chemical reaction given in Eq. (1), which justifies the choice of the variables  $a$  and  $c$  instead of  $a$  and  $b$ . Moreover, the mean value of the variable  $c$  is equal to the deterministic solution reducing to  $\bar{c} = 1$  for our choice of initial conditions.

In order to describe the internal noise, we deduce the Langevin forces from the master equation [17–19] governing the probability distribution for the stochastic processes  $a$  and  $c$ . In the master equation approach, the chemical reaction is modeled by birth and death processes and diffusion by a random walk. The Langevin force variances are identified with the second moments of the transition probability. It reads [19]

$$\begin{aligned} \langle F_a(x, y, t) F_a(x', y', t') \rangle \\ = \frac{\delta(t - t')}{\bar{C}} \left\{ K\bar{a}(1 - \bar{a})\delta(x - x')\delta(y - y') \right. \\ \left. + 2D\vec{\nabla} \cdot \vec{\nabla}' [\bar{a}\delta(x - x')\delta(y - y')] \right\}, \quad (14a) \end{aligned}$$

$$\begin{aligned} \langle F_c(x, y, t) F_c(x', y', t') \rangle \\ = \frac{2D}{\bar{C}} \delta(t - t') \vec{\nabla} \cdot \vec{\nabla}' [\delta(x - x')\delta(y - y')], \quad (14b) \end{aligned}$$

$$\begin{aligned} \langle F_a(x, y, t) F_c(x', y', t') \rangle \\ = \frac{2D}{\bar{C}} \delta(t - t') \vec{\nabla} \cdot \vec{\nabla}' [\bar{a}\delta(x - x')\delta(y - y')], \quad (14c) \end{aligned}$$

with

$$\vec{\nabla} = \begin{pmatrix} \frac{\partial}{\partial x} \\ \frac{\partial}{\partial y} \end{pmatrix}, \quad \vec{\nabla}' = \begin{pmatrix} \frac{\partial}{\partial x'} \\ \frac{\partial}{\partial y'} \end{pmatrix}$$

and where  $\bar{a} = \bar{a}(x, y, t)$  obeys the deterministic equation (4). Note that in addition to  $K$  and  $D$ , a third parameter, the mean total concentration  $\bar{C}$ , appears in the stochastic analysis. More precisely, the Langevin forces are proportional to  $1/\sqrt{\bar{C}}$ . The two systems defined by the parameter values given in Eq. (6) were associated with the same deterministic equation. Since  $\bar{C}_1 \neq \bar{C}_2$ , they are now de-

scribed by different Langevin equations.

The Langevin approach appears as a first order approximation of the master equation in the framework of a system-size expansion [17–19]. It corresponds to a Gaussian approximation that neglects irreducible transition probability moments of order higher than 2. The Langevin force variances given in Eqs. (14) define the noise statistics. At this order of approximation, the variables appearing in the expressions for the force variances may be replaced by their mean values, as has been done in Eq. (14).

For the sake of simplicity, a continuous description has been adopted up to now, but it is to be regarded as a convenient notation. As a matter of fact, the master equation formalism lays on a spatial discretization into cells. The choice of the cell size is a balance between two opposite constraints. On the one hand, the cells must be sufficiently small to be considered as homogeneous. On the other hand, a correct description of the chemical processes inside a cell requires sufficiently large cells, containing a large number of molecules so that the parameter  $\bar{C}$  obeys  $\bar{C} \gg 1$ . This justifies the system-size expansion in power of  $1/\sqrt{\bar{C}}$ .

As it is hopeless to look for an analytical solution of Eqs. (12) and (14), we solve them numerically. A discretized version of Eqs. (12) and (14), supported by the master equation approach and suitable for a numerical integration, is given in the Appendix. Using Eqs. (A6), we follow the evolution in time of the variables  $a_{ij}(t)$  and  $c_{ij}(t)$  in cell  $(i, j)$  of a two-dimensional square system. The system is divided in  $n$  by  $n$  cells with typically  $n = 512$  or  $n = 1024$ .

A plane initial condition with a steep profile is imposed. The simplest choice is a step function with  $a_{ij}(0) = 1$  for  $i \leq n/2$  and  $a_{ij}(0) = 0$  for  $i > n/2$  and with  $c_{ij}(0) = 1$ , whatever  $i$  and  $j$ . However, it is easy to look first for a numerical solution of the deterministic equation given in Eq. (4) for the same value of the parameters  $K$  and  $D$  than for the Langevin equations. We compute the stationary deterministic profile in the frame moving with the minimum velocity obeying Eq. (7). The initial choice of this deterministic profile, translated in the  $y$  direction labeled by  $j$  leads to the same asymptotic regime of the Langevin equations than the step function for a shorter computation time.

Classical periodic boundary conditions are imposed in the direction  $y$ , whereas the propagation of the front in

TABLE I. Comparison between deterministic and Langevin results in 1D and 2D media for different sizes of the system and for the following parameter values:  $K = 8 \times 10^{-4}$ ,  $D = 0.1$ , and  $\bar{C} = 100$ .

Results	Propagation velocity	Profile width	Number of cells
Deterministic equation	0.0179	89.5	512
1D Langevin equations	0.0220 ± 0.0002	110 ± 1	512 × 4
2D Langevin equations	0.0224 ± 0.0002	114 ± 1	512 × 512

the direction  $x$  is reproduced in the following manner. In order to mimic an infinite medium in the direction  $x$ , it is necessary to counterbalance the consumption of particles  $B$  due to the chemical reaction given by Eq. (1). To do so, the sum over all cells  $(i, j)$  of the fractions of particles  $A$  is compared with its initial value. More precisely, at each time step where the inequality

$$\sum_{i,j} a_{ij}(t) > \sum_{i,j} a_{ij}(0) \quad (15)$$

is obeyed, a procedure to reduce the  $A$  excess is started as follows:

- (i) the first column of cells, characterized by  $i=1$ , is suppressed;
- (ii) column  $i$ , for  $i \geq 2$ , becomes column  $i'=i-1$ ;
- (iii) a last column, characterized by  $i'=n$ , is created, in which  $a_{nj}(t)=0$ .

The front position denoted by  $\phi(t)$  is computed in the following manner: initially set equal to 0,  $\phi(t)$  is increased by 1 at each time step for which Eq. (15) is verified. The quantity  $\phi(t)$  contains global information about the entire front propagation and we define the front velocity  $v$  as the time derivative of the position  $\phi(t)$ .

Depending on the values of the three parameters  $K$ ,  $D$ , and  $\bar{C}$ , different asymptotic regimes are reached for which it is possible to define a mean stationary profile in the frame moving at velocity  $v$ . Hereafter, “mean” will refer to an average over the cells in direction  $j$  and over time  $t$ . It is then possible to characterize the steepness of this profile and to determine its width in the sense given in Eq. (8). Let us mention that our mean-front width definition differs from the one adopted by Chopard and Droz [7] from the position variance. Whereas the width defined in the latter work steadily increases in time, our choice allows us to compute a width that reaches a stationary value even in a fluctuating system and that can be quantitatively compared with the value predicted by the deterministic theory.

Typically, the integration of the Langevin equations given in Eqs. (A6) for a system of  $1024 \times 1024$  cells requires 1 s per time step on a CRAY YMP C98. For the parameter values listed in Tables I and II, the statistics needed after the stationary regime has been reached in the moving frame have required  $10^5$  time steps, which amounts to 30 h of computation time.

TABLE II. Same caption as Table I for the following parameter values:  $K=3 \times 10^{-4}$ ,  $D=0.1$ , and  $\bar{C}=100$ .

Results	Propagation velocity	Profile width	Number of cells
Deterministic equation	0.0110	146	1024
1D Langevin equations	$0.0142 \pm 0.0002$	$190 \pm 1$	$1024 \times 4$
2D Langevin equations	$0.0137 \pm 0.0002$	$185 \pm 1$	$1024 \times 1024$

#### IV. RESULTS DEDUCED FROM THE NUMERICAL INTEGRATION OF THE LANGEVIN EQUATIONS FOR THE FKPP MODEL

Our goal is to compare the values of the propagation velocity and the profile width predicted by the deterministic theory according to Eqs. (7) and (8) with the results deduced from the Langevin equations. Let us recall that the initial condition is a plane front whose profile in the direction  $x$  labeled by  $i$  is the deterministic solution propagating with the minimum velocity or any steeper profile. The Langevin equations given by Eqs. (A6) are integrated for given values of the three parameters  $K$ ,  $D$ , and  $\bar{C}$  over a sufficiently long time until a stationary regime is reached in the moving frame. The mean propagation velocity  $\langle v \rangle$  is a time average of the velocity deduced from the front position  $\phi(t)$  after the stationary regime has been reached. The mean width profile  $\langle e \rangle$  is deduced from the slope at the inflection point of the mean stationary profile.

The integration of the Langevin equations given in Eqs. (A6) in the case of a 2D medium can also be performed in a similar way in a 1D medium. The only change is to set apart the  $j$  label. In Tables I and II, we compare the results obtained in one-dimensional and two-dimensional systems. The mean propagation velocity and the mean profile width appear to be identical in 1D and 2D media, whatever the choice of the parameters  $K$ ,  $D$ , and  $\bar{C}$ . Taking advantage of this property, the computation time has been reduced by performing the following analysis in a one-dimensional system.

For fixed values of  $K$ ,  $D$ , and  $\bar{C}$ , we now study, in a 1D system, the influence of the length of the medium for which the Langevin equations are solved. In particular, we analyze the effect of the number of cells in front of the leading edge of the profile. Since the inflection point of the mean profile is stabilized in the middle cell, the number of cells in front of the leading edge doubles with the medium length. As shown in Table III, the mean propagation velocity, as well as the mean profile width, do not significantly vary with the medium length. Actually, in each case, we consider a sufficiently long medium, such that the fluctuating variable  $a(x, y, t)$  vanishes, up to the precision of the numerical computation, in an interval ranging from a given point of the leading edge up to the

TABLE III. Comparison between deterministic and Langevin results in 1D media for different lengths of the system and for the following parameter values:  $K=8 \times 10^{-4}$ ,  $D=0.1$ , and  $\bar{C}=100$ .

Results	Propagation velocity	Profile width	Number of cells
Deterministic equation	0.0179	89.5	
1D Langevin equations	$0.0220 \pm 0.0002$	$110 \pm 1$	$512 \times 4$
1D Langevin equations	$0.0226 \pm 0.0002$	$116 \pm 1$	$1024 \times 4$
1D Langevin equations	$0.0222 \pm 0.0002$	$112 \pm 1$	$2048 \times 4$

right boundary. In this interval, the Langevin force variances, proportional to the mean value  $\bar{a}(x, y, t)$  according to Eq. (14), also vanish, so that the state  $a=0$ , although unstable, cannot be destroyed by internal fluctuations. As a consequence, the effect of internal noise on the wave-front properties does not depend on the size of the interval for which  $a=0$ . Obviously, this property disappears when studying the effect of external noise [23], which enables the appearance of some nucleation germs of particles  $A$  in front of the leading edge of the profile.

Values listed in Tables I and II show that the mean quantities deduced from the Langevin equations are larger than the corresponding deterministic ones. For a concentration  $\bar{C}$  equal to 100, the discrepancy between deterministic and stochastic values for the propagation velocity as well as for the profile width reaches 25% with an error estimated around 1 or 2 %.

As appears from Eqs. (14), the  $\bar{C}$  parameter controls the amplitude of the Langevin force, and a systematic analysis of the velocity and width variations with  $\bar{C}$ , at fixed  $K$  and  $D$ , does reveal the influence of internal noise on wave-front propagation. The qualitative variations with  $\bar{C}$  of the profile width appear in Fig. 1. As  $\bar{C}$  increases, the noise term amplitude decreases, and the profile becomes steeper and tends to the deterministic profile associated with the minimum velocity. The time variations of the wall position in the fixed frame are given in Fig. 2 for different  $\bar{C}$  values. As  $\bar{C}$  increases, the slope of the profiles or (qualitatively) the front velocity decreases and tends to the minimum velocity predicted by the marginal stability analysis.

The quantitative variations with the Langevin force amplitude  $1/\sqrt{\bar{C}}$  of the mean profile width  $\langle e \rangle$  and of the mean velocity  $\langle v \rangle$  are respectively given in Figs. 3 and 4. The Langevin approach, whose validity relies on a

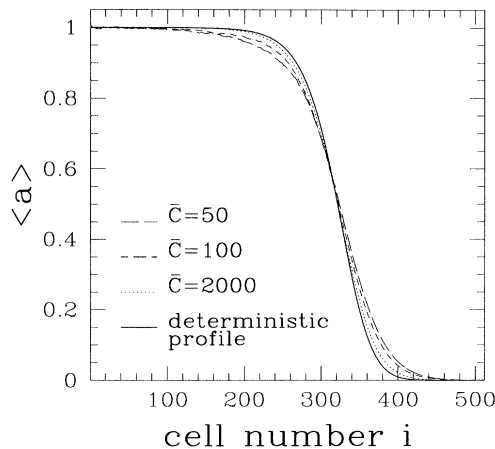


FIG. 1. Mean wave-front profiles, solutions of the Langevin equations, in the moving frame and for different values of the mean total concentration  $\bar{C}$ . Each curve represents the spatial variations in the propagation direction  $x$  labeled by  $i$  of the mean fraction  $\langle a \rangle$  of particles  $A$ . These results have been obtained for the parameter values  $K=8 \times 10^{-4}$ ,  $D=0.1$ , and in a system of  $512 \times 4$  cells, which can be considered as a 1D medium.

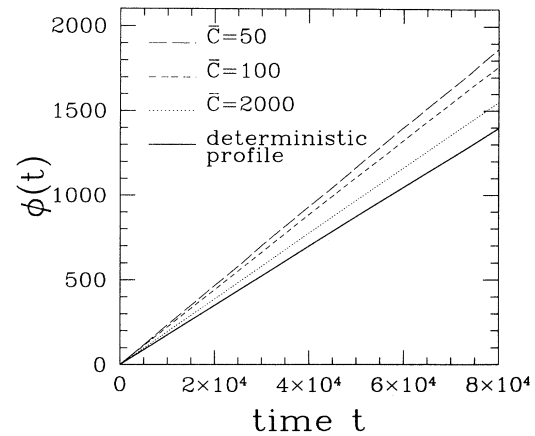


FIG. 2. Variations with time  $t$  of the front position  $\phi(t)$  in the fixed frame for different values of the mean total concentration  $\bar{C}$  and for the same parameter values as in Fig. 1.

system-size expansion in powers of  $1/\sqrt{\bar{C}}$  of the master equation, loses its sense for a too-high noise level. In practice, the results become meaningless for  $\bar{C} < 50$ . Inside this domain of validity, Figs. 3 and 4 clearly show the continuous increase of  $\langle e \rangle$  and  $\langle v \rangle$  with the noise level, i.e., with  $1/\sqrt{\bar{C}}$ .

To sum up, for given values of  $K$ ,  $D$ , and  $\bar{C}$ , the Langevin equations given in Eqs. (A6) admit a wave-front solution whose mean width and mean propagation velocity are greater than those predicted by the deterministic theory. The advantage of the Langevin formalism with respect to the microscopic simulations [10–12], which we undertook before, is to provide a parameter  $\bar{C}$  that controls the noise level independently of the other parameters  $K$  and  $D$ , allowing us to test if the deviation with deterministic results increases with the fluctuation amplitude. Such a systematic analysis was not possible in the microscopic simulations, since an increase of the noise level by the number density decrease was accompanied by

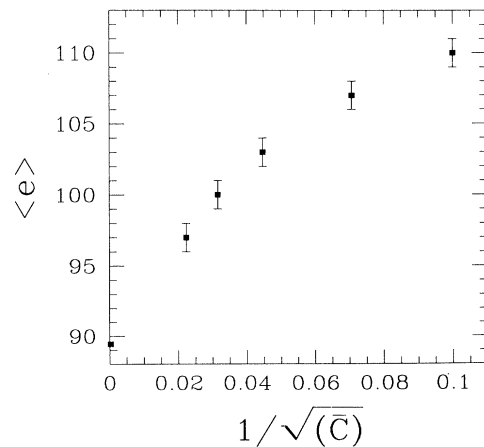


FIG. 3. Variations of the mean-front width  $\langle e \rangle$  with  $1/\sqrt{\bar{C}}$ , where  $\bar{C}$  is the mean total concentration and for the same parameter values as in Fig. 1.

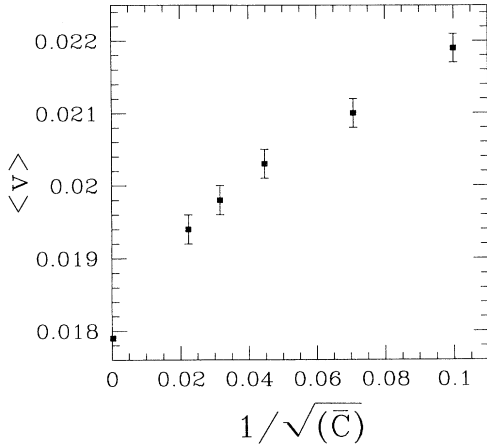


FIG. 4. Variations of the mean propagation velocity  $\langle v \rangle$  with  $1/\sqrt{\langle \bar{C} \rangle}$ , where  $\langle \bar{C} \rangle$  is the mean total concentration and for the same parameter values as in Fig. 1.

a variation of the diffusion coefficient  $D$ .

The continuous dependence of the mean-front properties with the noise level reveals that the deterministic solution is structurally stable with respect to stochastic perturbations induced by the underlying microscopic dynamics. Figure 5 shows a log-log plot of the variations with  $\langle \bar{C} \rangle$  of the difference  $\langle v \rangle - v_{\min}$  between the mean propagation velocity deduced from the Langevin equations and the minimum allowed velocity. The straight line of slope  $-\frac{1}{3}$  suggests the existence of the following scaling law:

$$\langle v \rangle - v_{\min} \propto \left[ \frac{1}{\sqrt{\langle \bar{C} \rangle}} \right]^{2/3}, \quad (16)$$

which proves that the deviation from the marginal stability analysis cannot be considered as a perturbation effect.

For given values  $K_0$  and  $D_0$  of the rate constant and of the diffusion coefficient, the deterministic profile

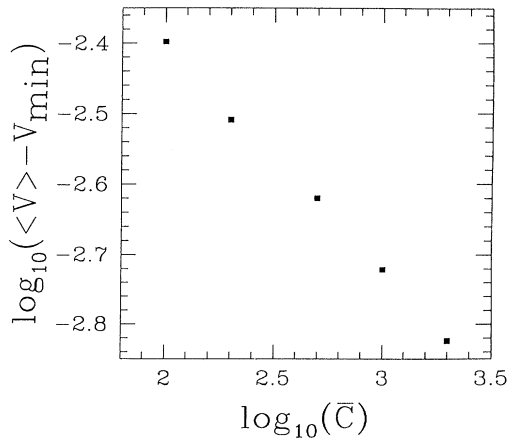


FIG. 5. Log-log plot of the variations with the mean total concentration  $\langle \bar{C} \rangle$  of the difference between the mean propagation velocity  $\langle v \rangle$  and the minimum allowed velocity  $v_{\min}$  for the same parameter values as in Fig. 1.

propagating with the minimum velocity  $v_{\min}^0 = 2\sqrt{K_0 D_0}$  as well as the mean solution of the Langevin equations associated with  $\langle \bar{C} \rangle = 1000$  have been represented in Fig. 6. As already mentioned, the mean stochastic solution has a larger width  $\langle e \rangle$  and propagates faster than the deterministic solution. The mean velocity of the fluctuating front is denoted by  $\langle v \rangle$ . A third profile has been added in Fig. 6; it is a deterministic solution associated with effective values  $K_1$  and  $D_1$  such that the profile has the same width,  $e_{\min}^1 \approx 8\sqrt{D_1/K_1}$ , and the same velocity,  $v_{\min}^1 = 2\sqrt{K_1 D_1}$ , than the Langevin profile. With our notations, it reads

$$e_{\min}^1 = \langle e \rangle, \quad v_{\min}^1 = \langle v \rangle. \quad (17)$$

By construction, the slopes at the inflection points of these two profiles are identical, but the mean stochastic profile is smoother in the leading edge region than the deterministic solution that has the same width. In order to compare more precisely these two profiles, we choose them as initial conditions and follow their deterministic evolution governed by Eq. (4) for the values  $K_0$  and  $D_0$  of the parameters; Eq. (4) is then numerically solved. For computational efficiency, we define an instantaneous profile width  $e'$  as the number of cells for which the fraction  $\bar{a}$  varies between 0.1 and 0.9. In Fig. 7, the deterministic evolution of the width  $e'$  is given in the case where the Langevin profile associated with  $K_0$  and  $D_0$ , as well as the deterministic effective profile associated with  $K_1$  and  $D_1$ , are chosen as initial conditions. Due to its definition, the width  $e'$  takes only integer values, which explains the discrete jumps in Fig. 7. At time  $t=0$  the

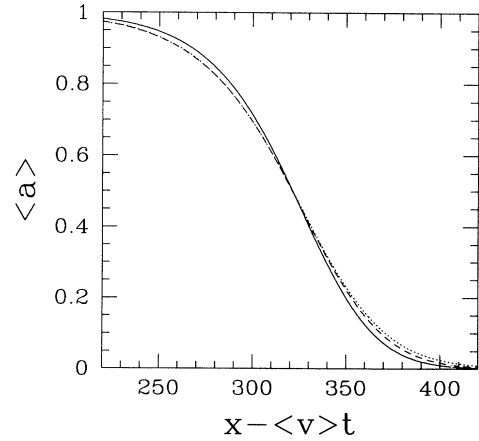


FIG. 6. Mean-front profiles in the moving frame. The solid line represents the deterministic profile propagating with the minimum velocity associated with  $K_0 = 8 \times 10^{-4}$  and  $D_0 = 0.1$ . The dotted line is the mean Langevin solution associated with  $\langle \bar{C} \rangle = 1000$  and the same values  $K_0$  and  $D_0$ . Its width  $\langle e \rangle$  and velocity  $\langle v \rangle$  are larger than the corresponding deterministic values. The dashed line is the effective deterministic profile propagating with the same velocity and having the same width as the Langevin solution. It is associated with the parameter values  $K_1 = 7.92 \times 10^{-4}$  and  $D_1 = 0.1238$  that have been chosen in such way that  $v_{\min}^1 = 2\sqrt{K_1 D_1} = \langle v \rangle$  and  $e_{\min}^1 \approx 8(D_1/K_1)^{1/2} = \langle e \rangle$ .

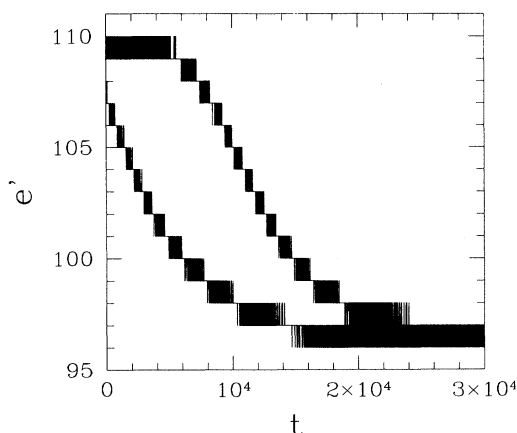


FIG. 7. Deterministic temporal evolutions of the profile width  $e'$  defined as the number of cells for which the fraction  $\bar{u}$  varies between 0.1 and 0.9. The two curves are deduced from the numerical integration of the deterministic equation associated with  $K_0 = 8 \times 10^{-4}$  and  $D_0 = 0.1$  for two different initial conditions. The upper curve is obtained when the asymptotic mean solution of the Langevin equations associated with the same values  $K_0$  and  $D_0$  is initially chosen. The lower curve is obtained when the initial profile is the deterministic solution associated with the effective parameter values  $K_1 = 7.92 \times 10^{-4}$  and  $D_1 = 0.1238$ .

width  $e'$  of the deterministic profile is smaller than those of the Langevin profile, in agreement with the behavior in the leading edge already observed in Fig. 6.

More important, it appears that, when the deterministic profile associated with  $K_1$  and  $D_1$  is initially chosen, the width of the deterministic solution rapidly decreases to reach an asymptotic value, exhibiting the rapid relaxation of the profile towards the marginal stability solution associated with  $K_0$  and  $D_0$ . On the contrary, when the Langevin profile is the initial condition, the width  $e'$  remains unchanged during a relatively long time. The existence of such a plateau in the evolution of the profile width reflects the deterministic stability of the solution selected by the Langevin equation. However, the profile finally relaxes to the solution propagating with the minimum velocity. It is to be noted that the length of the plateau is sensitive to the precision of the numerical computation. In particular, the minimization of unavoidable numerical errors by the choice of a smaller time step in the integration of Eq. (4) increases the length of the plateau, i.e., the time during which the Langevin profile remains a solution of the deterministic equation.

The numerical integration of the Langevin equations clearly shows that the effect of internal noise is to increase the propagation velocity as well as the profile width of the wave front. Moreover, we think, on the one hand, that the existence of a plateau in Fig. 7 indicates that the mean solution of the Langevin equations is a particular deterministic wave front that has been selected by internal noise in the continuum of possible solutions of the deterministic equation. On the other hand, the final relaxation towards the marginal stability solution observed in Fig. 7 shows that (external) noise induced by

small uncontrolled numerical errors destroys the fronts associated with greater velocities than  $v_{\min}$ . This last phenomenon exhibits the specific role played by the internal noise.

## V. CONCLUSION

The FKPP equation is the prototype reaction-diffusion equation admitting wave-front solutions propagating into an unstable state. The main feature of this type of wave fronts is the existence of a continuum of possible propagation velocities. Suspecting the important role that internal noise could play on such a degenerate state, we have used the Langevin formalism to take into account the internal fluctuations generated by the underlying microscopic dynamics. The expression of the Langevin forces is deduced from a first-order approximation of the master equation in the framework of a system-size expansion.

We found that the mean wave-front solutions of the Langevin equations have a larger width and propagate faster than the corresponding deterministic solutions. The Langevin formalism provides an independent parameter, the mean total concentration  $\bar{C}$ , which controls the internal noise level. To remain in the validity domain of the system-size expansion in powers of  $1/\sqrt{\bar{C}}$ , it is not possible to increase the noise level indefinitely. We observe a systematic increase of the mean width and the mean propagation velocity  $\langle v \rangle$  as  $1/\sqrt{\bar{C}}$  increases. The discrepancy between stochastic and deterministic values reaches 25% for the highest noise level available.

The effect of internal fluctuations is thus to select a propagation velocity greater than the minimum allowed velocity  $v_{\min}$ , in contradiction with the marginal stability analysis. The scaling law observed,  $\langle v \rangle - v_{\min} \propto (1/\sqrt{\bar{C}})^{2/3}$ , suggests that this effect cannot be considered as a perturbation. Taking into account the stability properties of the mean Langevin profile when it is chosen as an initial condition for the deterministic equation, we conjecture that the effect of internal noise is to select a particular wave front in the continuum of possible deterministic solutions. Similar results have been recently obtained by Peeters and Baras [24] from the numerical integration of the corresponding master equation. To test the validity of our conjecture, we plan to determine if this important fluctuation effect is specific to wave fronts propagating into an unstable state. In particular, we wish to compare the behavior of the FKPP model with a reaction-diffusion model admitting wave fronts propagating between two stable stationary states: such behavior is found, for example, in the Schlögl model [25]. Up to now, the internal noise effect analysis is purely numerical, and some analytical work would be welcome.

## ACKNOWLEDGMENTS

We wish to thank Dr. M. Malek-Mansour for his efficient help concerning the numerical integration of the Langevin equations. This work was possible thanks to the support of the Institut de Développement et des Ressources en Informatique Scientifique (IDRIS, Orsay, France).

## APPENDIX

In this appendix, the discretized form of the stochastic differential equations associated with the FKPP model is deduced; the continuous version is given by Eqs. (12) and (14). The contribution of chemistry to the noise term, labeled by the subscript  $K$ , and those of diffusion, labeled by the subscript  $D$ , may be separated in Eqs. (12) and (14), leading to the following equations:

$$\frac{\partial a}{\partial t} = Ka(c-a) + D \left[ \frac{\partial^2 a}{\partial x^2} + \frac{\partial^2 a}{\partial y^2} \right] + F_a^K(x, y, t) + \vec{\nabla} \cdot \vec{F}_a^D(x, y, t), \quad (\text{A1})$$

$$\frac{\partial c}{\partial t} = D \left[ \frac{\partial^2 c}{\partial x^2} + \frac{\partial^2 c}{\partial y^2} \right] + \vec{\nabla} \cdot \vec{F}_c^D(x, y, t),$$

where the Langevin-force variances obey

$$\begin{aligned} \langle F_a^K(x, y, t) F_a^K(x', y', t') \rangle \\ = \frac{K}{C} \bar{a} (1 - \bar{a}) \delta(x - x') \delta(y - y') \delta(t - t'), \end{aligned} \quad (\text{A2})$$

$$\begin{aligned} \langle \vec{\nabla} \cdot \vec{F}_\alpha^D(x, y, t) \vec{\nabla}' \cdot \vec{F}_\alpha^D(x', y', t') \rangle \\ = \frac{2D}{C} \delta(t - t') \vec{\nabla} \cdot \vec{\nabla}' [\bar{a} \delta(x - x') \delta(y - y')] \end{aligned}$$

for  $\alpha$  equal to  $a$  or  $c$ ,

$$\begin{aligned} \langle \vec{\nabla} \cdot \vec{F}_a^D(x, y, t) \vec{\nabla}' \cdot \vec{F}_c^D(x', y', t') \rangle \\ = \frac{2D}{C} \delta(t - t') \vec{\nabla} \cdot \vec{\nabla}' [\bar{a} \delta(x - x') \delta(y - y')]. \end{aligned}$$

The chemical noise  $F^K$  and the diffusive noise  $\vec{\nabla} \cdot \vec{F}^D$  are independent. Note that the diffusive noise couples the evolution of the variables  $a$  and  $c$  and that it induces non-trivial spatial correlations.

Dividing space  $(x, y)$  into square cells of side  $\Delta l$  and denoting by  $\Delta t$  the integration time step, we define discrete space and time variables by

$$i = x/\Delta l, \quad j = y/\Delta l, \quad s = t/\Delta t, \quad (\text{A3})$$

where  $i, j$ , and  $s$  are integers.

We introduce dimensionless parameters  $k, d$ , and  $\gamma$  as follows. The parameters  $k$  and  $d$  are respectively deduced from the kinetic constant and the diffusion coefficient appearing in Eq. (12) by

$$k = K \Delta t, \quad d = \frac{D \Delta t}{(\Delta l)^2}, \quad (\text{A4})$$

and  $\gamma$ , defined as the mean total number of particles in a cell, obeys

$$\gamma = \bar{C} (\Delta l)^2. \quad (\text{A5})$$

It is convenient to choose time and length units such that  $\Delta t = 1$  and  $\Delta l = 1$ . Using the notations introduced above, the discrete version of Eqs. (A1) and (A2) yields

$$\begin{aligned} a_{ij}(s+1) &= a_{ij}(s) + k a_{ij}(c_{ij} - a_{ij}) + d(a_{i+1j} + a_{i-1j} + a_{ij+1} + a_{ij-1} - 4a_{ij}) + \sqrt{k/\gamma} \sqrt{\bar{a}_{ij}(1 - \bar{a}_{ij})} Z_{ij}(s) \\ &\quad + \sqrt{d/\gamma} \{ \sqrt{\bar{a}_{i-1j} + \bar{a}_{-ij}} X_{ij}^a(s) - \sqrt{\bar{a}_{ij} + \bar{a}_{i+1j}} X_{i+1j}^a(s) + \sqrt{2\bar{a}_{ij}} [Y_{ij}^a(s) - Y_{ij+1}^a(s)] \}, \\ c_{ij}(s+1) &= c_{ij}(s) + d(c_{i+1j} + c_{i-1j} + c_{ij+1} + c_{ij-1} - 4c_{ij}) \\ &\quad + \{ \sqrt{d/\gamma} \sqrt{\bar{a}_{i-1j} + \bar{a}_{ij}} X_{ij}^a(s) - \sqrt{\bar{a}_{ij} + \bar{a}_{i+1j}} X_{i+1j}^a(s) + \sqrt{2\bar{a}_{ij}} [Y_{ij}^a(s) - Y_{ij+1}^a(s)] \} \\ &\quad + \sqrt{d/\gamma} \{ \sqrt{2 - \bar{a}_{i-1j} - \bar{a}_{ij}} X_{ij}^b(s) - \sqrt{2 - \bar{a}_{ij} - \bar{a}_{i+1j}} X_{i+1j}^b(s) + \sqrt{2(1 - \bar{a}_{ij})} [Y_{ij}^b(s) - Y_{ij+1}^b(s)] \}, \end{aligned} \quad (\text{A6})$$

where  $X_{ij}^\alpha(s)$ ,  $Y_{ij}^\alpha(s)$ , and  $Z_{ij}(s)$  are independent Gaussian white noises of zero mean and unit variances, obeying in particular

$$\langle X_{ij}^\alpha(s) X_{i'j'}^\beta(s') \rangle = \delta_{\alpha\beta} \delta_{ii'} \delta_{jj'} \delta_{ss'}, \quad (\text{A7})$$

with  $\alpha$  and  $\beta$  taking the value  $a$  or  $b$ .

The complexity of Eqs. (A6) is partly due to the spatial coupling of the noises induced by diffusion. Actually, the evolution in cell  $(i, j)$  is coupled through the diffusive

noise term to the evolution of its nearest neighbors  $(i \pm 1, j)$  and  $(i, j \pm 1)$ . From a technical point of view, the numerical resolution of Eqs. (A6) implies the generation of a large amount of random numbers in a Gaussian distribution, five times the number of cells at each time step, exactly. Moreover, the existence of correlations requires the storage of these numbers. Even after optimization, the time consuming part of the program remains the generation of Gaussian random numbers itself.

- [1] R. A. Fischer, *Ann. Eugenics* **7**, 335 (1937).  
 [2] A. Kolmogorov, I. Petrovsky, and N. Piskunov, *Bull. Univ. Moscow. Ser. Intl. Sec. A* **1** (6), 1 (1937).  
 [3] J. D. Murray, *Mathematical Biology* (Springer, Berlin, 1989).  
 [4] Y. B. Zeldovich and G. I. Barenblatt, *Combust. Flame* **3**,

- 61 (1959).  
 [5] A. R. Kerstein, *J. Stat. Phys.* **53**, 703 (1988).  
 [6] G. C. Paquette, *Phys. Rev. A* **44**, 6577 (1991).  
 [7] B. Chopard and M. Droz, *Europhys. Lett.* **15**, 459 (1991).  
 [8] S. Cornell, M. Droz, and B. Chopard, *Phys. Rev. A* **44**, 4826 (1991).



- [9] B. Chopard, M. Droz, T. Karapiperis, and Z. Racz, *Phys. Rev. E* **47**, R40 (1993).
- [10] A. Lemarchand, H. Lemarchand, E. Sulpice, and M. Mareschal, *Physica A* **188**, 227 (1992).
- [11] A. Lemarchand, A. Lesne, A. Perera, M. Moreau, and M. Mareschal, *Phys. Rev. E* **48** 1568 (1993).
- [12] A. Lemarchand, H. Lemarchand, A. Lesne, and M. Mareschal, in *Far From Equilibrium Dynamics of Chemical Systems III*, edited by J. Gorecki *et al.* (World Scientific, Singapore, 1994).
- [13] D. G. Aronson and H. F. Weinberger, *Adv. Math.* **30**, 33 (1978).
- [14] P. Fife, *Mathematical Aspects of Reacting and Diffusing Systems*; edited by S. Levin, *Lecture Notes in Biomathematics* Vol. 28 (Springer, New York, 1979).
- [15] W. van Saarloos, *Phys. Rev. Lett.* **58**, 2571 (1987); *Phys. Rev. A* **37**, 211 (1988); **39**, 6367 (1989).
- [16] L. Y. Chen, N. Goldenfeld, Y. Oono, and G. Paquette, *Physica A* **204**, 111 (1994).
- [17] G. Nicolis and I. Prigogine, *Self-Organization of Non-Equilibrium Systems* (Wiley, New York, 1977).
- [18] N. G. van Kampen, *Stochastic Processes in Physics and Chemistry* (North-Holland, Amsterdam, 1981).
- [19] G. W. Gardiner, *Handbook of Stochastic Methods* (Springer, Berlin, 1985).
- [20] L. Frachebourg, Ph. D. thesis, Université de Genève, 1994 (unpublished).
- [21] G. A. Bird, *Molecular Gas Dynamics and the Direct Simulation of the Gas Flows* (Clarendon, Oxford, 1994).
- [22] J. Hardy, O. de Pazzis, and Y. Pomeau, *Phys. Rev. A* **13**, 1949 (1976).
- [23] G. F. Mazenko, O. T. Valls, and P. Ruggiero, *Phys. Rev. B* **40**, 384 (1989).
- [24] P. Peeters and F. Baras (unpublished).
- [25] F. Schlögl, C. Escher, and R. S. Berry, *Phys. Rev. A* **27**, 2698 (1983).